

Spatial distribution of lost ripple-trapped suprathermal electrons.

F. Medina, M. A. Ochando, A. Baciero and J. Guasp

Laboratorio Nacional de Fusión. Asociación EURATOM/CIEMAT, 28040 Madrid, Spain

Introduction

The ECRH driven convective flux of ripple-trapped suprathermal electrons in low density stellarator plasmas has been mentioned as being related to various features and phenomena: the suprathermal feature and the burst-like phenomena in the ECE emissions [1], the electron-root feature [2] and the phenomenon of electric pulsation [3]. In a previous investigation on TJ-II plasmas [4], fast transitions in confinement regimes were found to be associated to changes in the electron distribution function and to changes in the direct convective losses at the heating region. There, low order rational surfaces located at the gradient region seemed to be affecting the trapping/de-trapping rates. It was also reported [5] that the plasma potential at the core region increased with the characteristic energy of the electron suprathermal electron tail.

Here we present the spatial distribution of electron losses to the vacuum vessel and to the graphite limiter detected through their bremsstrahlung emission in the range of the soft x rays. Electron losses are monitored with the **SXR tomography diagnostic**, using thick Be filters to reduce the contribution of plasma emission, and a **planar Ge detector** to obtain the spectra [6], see Fig. 1 and 2.

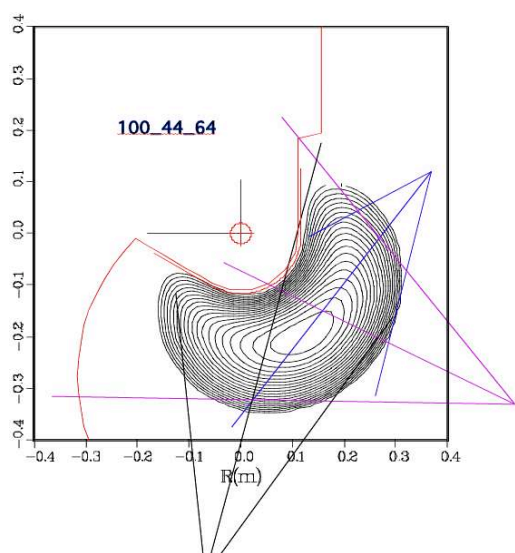


Fig. 1. Schematic view of the tree inner SXR cameras.

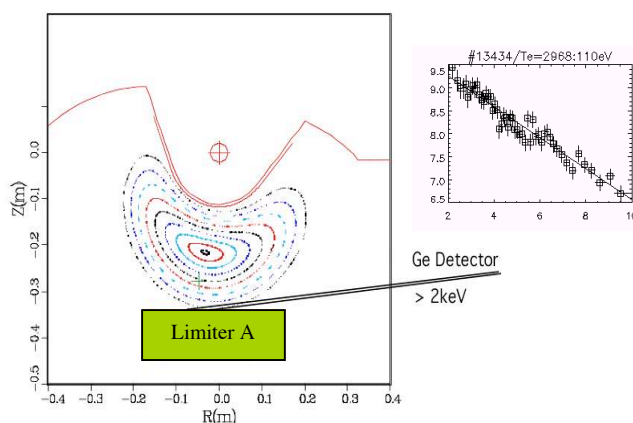


Fig. 2. Schematic view of the Ge detector location and a typical spectrum in the range of 2 keV to 10 keV

Results

Three distinct losses regions were observed at the inboard side of the vessel wall. The emissions coming from each of them behave differently with electron density, heating method (ECR on-axis vs. off-axis) and Z_{eff} . The experiments were carried out, in steady state plasmas as well as in plasmas showing transitions between different confinement regimes.

The SXR spectra in TJ-II at the plasma core usually present a suprathermal component, with characteristic energies ranging from two to four times the central T_e , when measured in the range of 4 keV to 10 keV. This ECRH generated suprathermal electrons have now been detected at the vacuum vessel and at the limiter, and their emission spectra show only the suprathermal component. The thermal component that, at plasma core, dominates the spectra in the range of 1 keV to 4 keV is absent.

Fast transitions in the plasma core, as observed by the ECE channels and central SXR chords, have an instantaneous response in the signal levels of direct losses. An increase of ECE signals is accompanied with a reduction in the plasma centre SXR emission, as a consequence of a decrease of plasma density, and also a sharp increase in the monitors of direct losses both, at the vacuum vessel and at the limiter (see Fig. 3).

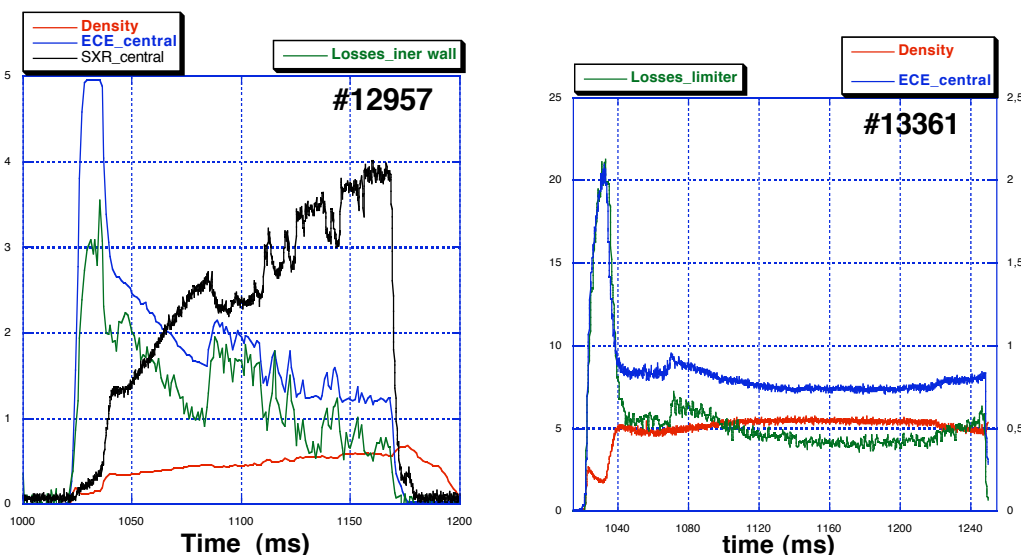


Fig. 3. Fast transitions at the plasma core as observed at (left) plasma wall and (right) the limiter.

TJ-II has two equivalent limiters. By observing the direct losses on limiter A, while radially scanning the limiter C, there was observed no reduction in the monitor signals. This shows that the electrons that originate the emissions do not circulate the torus, they are trapped in the TJ-II helical magnetic field ripple (see Fig. 4).

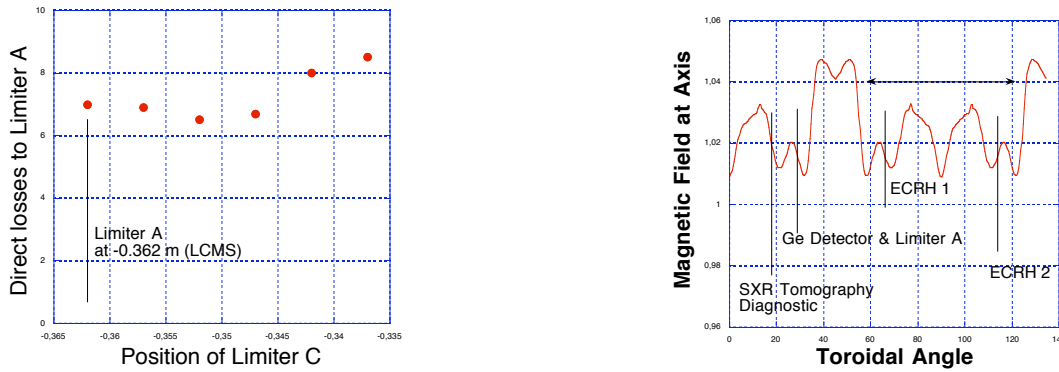


Fig. 4. (left), Intensity of direct losses at limiter A while introducing the limiter C inside the plasma. (right), Magnetic field at axis. Also shown the diagnostic and the microwave injection ports positions.

As expected, the observed direct losses intensity scales inversely proportional with density: an increase of density, at constant input power, means a decrease of power density and therefore a reduction in the deformation of the electron distribution function. This is also observed as a reduction of the characteristic energy in the spectra (see Fig. 5).

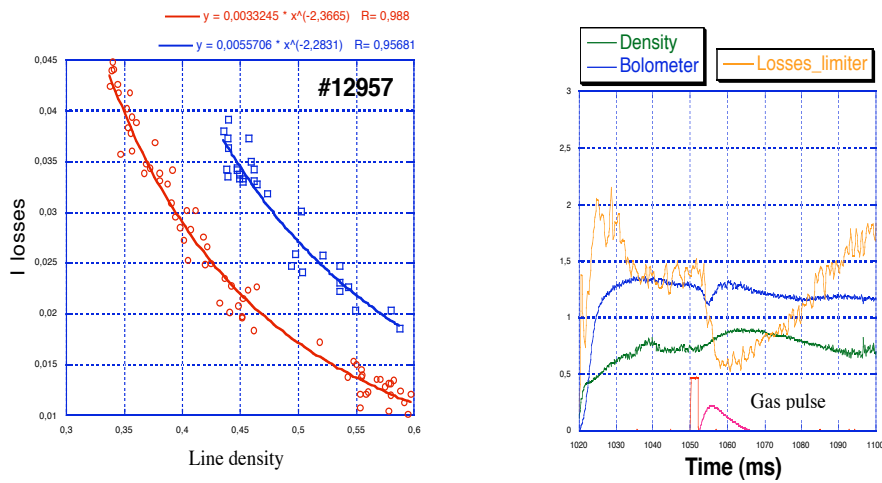


Fig. 5. (left), Density dependence for the shot in Fig. 3 (left), the two confinements regimes are treated separately. (right), Time evolution after a short pulse of gas injection.

When microwaves are launched off-axis a two-fold increment of direct losses is observed. Although off-axis would mean a reduction of the power density, because of a wider area of power deposition, the possibility of microwave absorption away from magnetic axis could explain the result. Also, the poloidal distribution of direct losses to the wall is greatly modified (see Fig. 6). While three different bands are observed in on-axis heated plasmas, in off-axis heated plasmas one band is absent and another is shifted. Variation in the electrons pitch angle and the radial electric field could explain the existence of these bands and their dependence with the heating conditions.

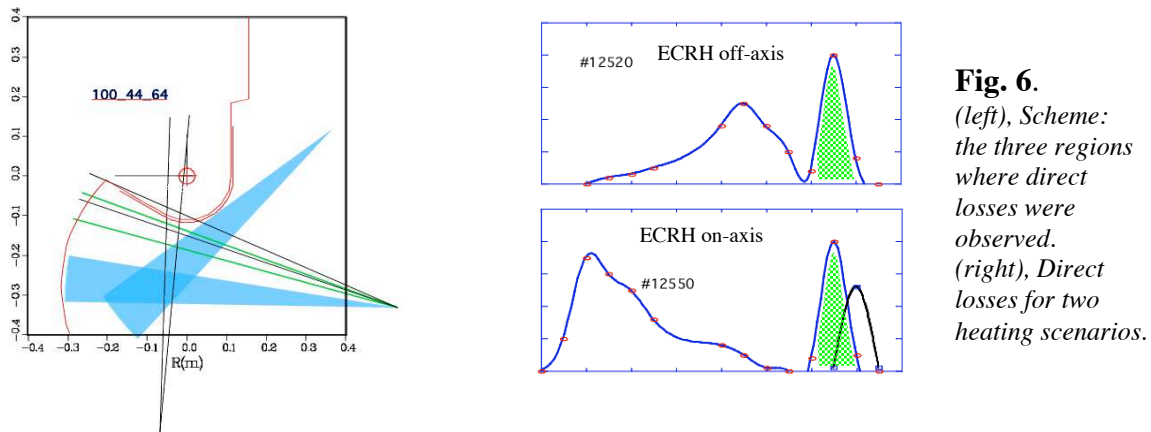


Fig. 6. (left), Scheme: the three regions where direct losses were observed. (right), Direct losses for two heating scenarios.

The dependence of direct losses with Z_{eff} is counterintuitive: an increase of plasma collisionality should reduce the electron distribution function deformation and therefore the direct losses. However, there are previous observations indicating that direct losses in TJ-II are toroidally asymmetric [4].

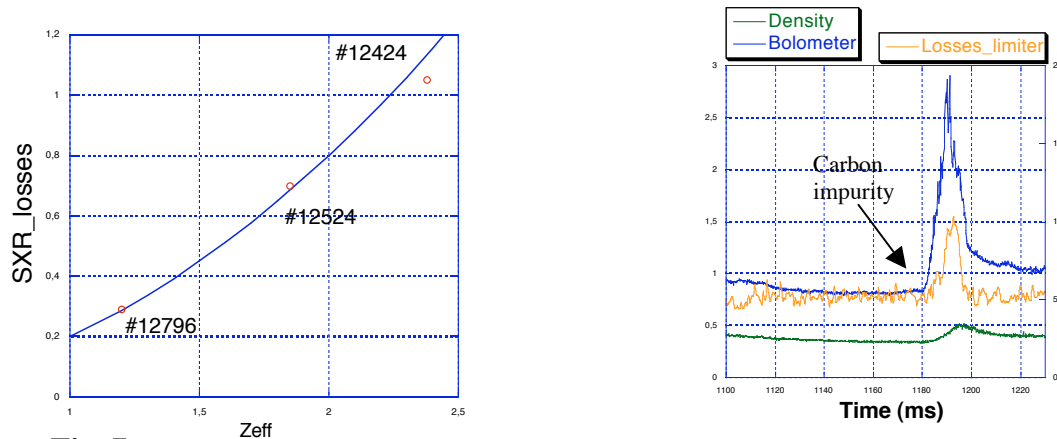


Fig. 7. (left), Dependence of direct losses to the wall as a function of Z_{eff} for three discharges with identical average electron line density. (right), Time evolution after sudden entrance of carbon.

The increase of the observed direct losses could be the result of a double collisional process. As a result of an increase of collisionality more electrons could be pumped away, “untrapped”, from the magnetic wells close to the microwave injection ports, being then, susceptible to be trapped again in the helical ripples where they are finally observed (see Fig. 4 right). Notice that, if this hypothesis were confirmed, the so far monitored direct losses would be just a minor fraction of the total. To confirm this hypothesis a new detector will be installed near the microwave injection ports.

References

- [1] Romé M et al 1997 Plasma Phys. Control. Fusion 39 117
- [2] Kick M et al 1999 Plasma Phys. Control. Fusion 41 A549
- [3] Fujisawa A et al. 1999 Plasma Phys. Control. Fusion 41 A561
- [4] Ochando M A and Medina F et al 2003 Plasma Phys. Control. Fusion 45 221
- [5] Medina F. et al Proc. 31st EPS (London 2004)
- [6] Medina F. et al, RSI 1999